Production asymmetry of D$_s$ from 600 GeV/c Σ$^-$ and π$^-$ beam

SELEX Collaboration

M. Kaya [p,5], G. Alkhazov [k], A.G. Atamantchouk [k,1], M.Y. Balatz [h,1], N.F. Bondar [k],
P.S. Cooper [e], L.J. Dauwe [q], G.V. Davidenko [h], U. Dersch [i,2], A.G. Dolgolenko [h],
G.B. Dzyubenko [h], R. Edelstein [c], L. Emediato [s], A.M.F. Endler [d], J. Engelfried [m,e],
I. Eschrich [i,3], C.O. Escobar [s,4], A.V. Evdokimov [h], I.S. Filimonov [j,1], F.G. Garcia [s,e],
M. Gaspero [r], I. Giller [l], V.L. Golovtsov [k], P. Gouffon [s], E. Gülmez [b], He Kangling [g],
M. Iori [r], S.Y. Jun [c], J. Kilmer [e], V.T. Kim [k], L.M. Kochenda [k], I. Konorov [i,6],
A.P. Kozhevnikov [f], A.G. Krivshich [k], H. Krüger [i,7], M.A. Kubantsev [h],
V.P. Kubarovsky [f], A.I. Kulyavtsev [c,e], N.P. Kuropatkin [k,e], V.F. Kurshetsov [f],
A. Kushnirenko [c], S. Kwan [e], J. Lach [e], A. Lamberto [t], L.G. Landsberg [f], I. Larin [h],
E.M. Leikin [j], Li Yunshan [g], M. Luksys [n], T. Lungov [s,8], V.P. Maleev [k], D. Mao [c,9],
Mao Chensheng [g], Mao Zhenlin [g], P. Mathew [c,10], M. Mattson [c], V. Matveev [h],
E. McCliment [p], M.A. Moinester [l], V.V. Molchanov [f], A. Morelos [m], K.D. Nelson [p,11],
A.V. Nemitkin [j], P.V. Neoustroev [k], C. Newsom [p], A.P. Nilov [h], S.B. Nurushev [f],
A. Ocherashvili [l], Y. Onel [p], E. Ozel [p], S. Ozkorucuklu [p], A. Penzo [t], S.V. Petrenko [f],
P. Pogodin [p], M. Procario [c,12], V.A. Prutskoi [h], E. Ramberg [e], G.F. Rappazzo [t],
B.V. Razmyslovich [k,13], V.I. Rud [j], J. Russ [c], P. Schiavon [t], J. Simon [i,14], A.I. Sitnikov [h],
D. Skow [e], V.J. Smith [o], M. Srivastava [s], V. Steiner [l], V. Stepanov [k,13], L. Stutte [e],
M. Svoiski [k,13], N.K. Terentyev [k,c], G.P. Thomas [a], L.N. Uvarov [k], A.N. Vasiliev [f],
D.V. Vavilov [f], V.S. Verebryusov [h], V.A. Victorov [f], V.E. Vishnyakov [h], A.A. Vorobyov [k],
K. Vorwalter [i,15], J. You [c,e], Zhao Wenheng [g], Zheng Shuchen [g], R. Zukanovich-Funchal [s]

[a] *Ball State University, Muncie, IN 47306, USA*
[b] *Bogazici University, Bebek 80815 Istanbul, Turkey*
[c] *Carnegie-Mellon University, Pittsburgh, PA 15213, USA*
[d] *Centro Brasileiro de Pesquisas Físicas, Rio de Janeiro, Brazil*
[e] *Fermi National Accelerator Laboratory, Batavia, IL 60510, USA*
[f] *Institute for High Energy Physics, Protvino, Russia*
[g] *Institute of High Energy Physics, Beijing, PR China*
[h] *Institute of Theoretical and Experimental Physics, Moscow, Russia*
[i] *Max-Planck-Institut für Kernphysik, 69117 Heidelberg, Germany*
[j] *Moscow State University, Moscow, Russia*
[k] *Petersburg Nuclear Physics Institute, St. Petersburg, Russia*
[l] *Tel Aviv University, 69978 Ramat Aviv, Israel*
[m] *Universidad Autónoma de San Luis Potosí, San Luis Potosí, Mexico*

[n] *Universidade Federal da Paraíba, Paraíba, Brazil*
[o] *University of Bristol, Bristol BS8 1TL, United Kingdom*
[p] *University of Iowa, Iowa City, IA 52242, USA*
[q] *University of Michigan-Flint, Flint, MI 48502, USA*
[r] *University of Rome "La Sapienza" and INFN, Rome, Italy*
[s] *University of São Paulo, São Paulo, Brazil*
[t] *University of Trieste and INFN, Trieste, Italy*

Abstract

The production of D_s^- relative to D_s^+ as a function of x_F with 600 GeV/c Σ^- beam is measured in the interval $0.15 < x_F < 0.7$ by the SELEX (E781) experiment at Fermilab. The integrated charge asymmetries with 600 GeV/c Σ^- beam (0.53 ± 0.06) and π^- beam (0.06 ± 0.11) are also compared. The results show the Σ^- beam fragments play a role in the production of D_s^-, as suggested by the leading quark model.
© 2003 Elsevier Science B.V. All rights reserved.

1. Introduction

Perturbative Quantum Chromodynamics calculations in leading or next-to-leading order predict very small or no asymmetry in the x_F or p_t distributions for charm and anticharm production [1,2]. However, fixed target data show some asymmetry between the production of some charm and anticharm hadrons in hadron-hadron interactions [3,4]. SELEX has shown strong,

---

E-mail address: yasar-onel@uiowa.edu (Y. Onel).

[1] Deceased.

[2] Present address: Infinion, München, Germany.

[3] Present address: Imperial College, London SW7 2BZ, UK.

[4] Present address: Instituto de Física da Universidade Estadual de Campinas, UNICAMP, SP, Brazil.

[5] Present address: Kafkas University, Kars, Turkey.

[6] Present address: Physik-Department, Technische Universität München, 85748 Garching, Germany.

[7] Present address: The Boston Consulting Group, München, Germany.

[8] Present address: Instituto de Física Teórica da Universidade Estadual Paulista, São Paulo, Brazil.

[9] Present address: Lucent Technologies, Naperville, IL, USA.

[10] Present address: SPSS Inc., Chicago, IL, USA.

[11] Present address: University of Alabama at Birmingham, Birmingham, AL 35294, USA.

[12] Present address: DOE, Germantown, MD, USA.

[13] Present address: Solidum, Ottawa, Ontario, Canada.

[14] Present address: Siemens Medizintechnik, Erlangen, Germany.

[15] Present address: Deutsche Bank AG, Eschborn, Germany.

beam-dependent asymmetries in Λ_c^+ production [5]. This experiment finds that $D_s^\pm$ production from a Σ^- beam (but not a π^- beam) also has a large production asymmetry. This asymmetry could be due to the fact that the beam hadron shares a quark with one of the charge states (hence leading particle) and not with the other charge state (non-leading). This is sometimes called "the leading particle effect".

For a $\Sigma^-(sdd)$ beam the $D_s^-(\bar{c}s)$ shares an s quark with the beam hadron and is a leading particle, whereas $D_s^+(c\bar{s})$ is not. For a $\pi^-(\bar{u}d)$ beam, neither D_s^- nor D_s^+ is leading. Several theoretical models have been proposed to explain charm hadroproduction in the framework of non-perturbative hadronization. Among the proposed models are the color-drag string model [6], which is pronounced at high x_F and is independent of p_t, and the intrinsic charm model [7], which manifests itself at low p_t and larger x_F.

2. Apparatus

Data were taken during the 1996–1997 fixed target run at Fermilab. The 600 GeV/c negative hadron beam used in this measurement was composed of approximately 50% Σ^- and 50% π^-. Beam particles were tagged with a transition radiation detector system located upstream of the charm production target.

A segmented target consisting of two copper sheets and three diamond sheets, each spaced by 1.5 cm, was used to produce charm particles. The total target thickness was 4.2% of an interaction length for protons.

The SELEX experiment used a three-stage spectrometer designed for large acceptance at $x_F > 0.1$ and for detecting the decay of charm particles. Each stage included a bending magnet and a detector system.

SELEX used an online trigger to identify charm particles. The hardware trigger required at least 4 charged hadrons in the forward 150 mrad cone and 2 hits from positive track candidates in a hodoscope after second magnet (M2). The software trigger made a full vertex reconstruction of the beam track and all tracks in the M2 spectrometer. Trigger conditions were also included in the simulation.

The RICH detector, located after the second spectrometer system, was filled with neon gas at room temperature and 1.05 atm pressure. It identified charged hadrons whose trajectories went through the fiducial volume, typically requiring $p > 23$ GeV/c [8]. Full reconstruction of the secondary vertex was provided by linking RICH-identified tracks back through the second stage magnetic spectrometer to the vertex silicon detector and associating them at a common decay vertex downstream of the primary interaction vertex.

3. Data analysis

Initial data selection required two kaons to be identified by the RICH (ratio of the likelihoods: $\mathcal{L}(K)/\mathcal{L}(\pi) \geqslant 1$) and the primary vertex to be in a target sheet.

The criteria used to select D_s candidates included the following cuts:

 (i) Secondary vertex separation significance $L/\sigma > 9$ where L is the longitudinal separation between primary and secondary vertex and σ is the error on L.
 (ii) Secondary vertex was at least 100 microns outside of the target material.
(iii) Each secondary track was extrapolated back to primary vertex z-position to evaluate the transverse miss distance b. The second largest miss distance had to have $(b/\sigma_b)^2 > 8$, where σ_b is the error on b.

These cuts were chosen to reject as many background events as possible without losing too much signal. They were optimized using real background and simulated signal events by maximizing the so-called significance: $S/\sqrt{N_s + N_b}$ where S was the yield from a Monte Carlo data set. The numbers of signal (N_s) and background (N_b) events inside the square root were taken from data (all the events within the mass interval of 50 MeV/c^2 centered at D_s mass value). The cuts are identical for the charge conjugate modes. None of the results presented here is sensitive to this optimization procedure.

Since the RICH detector does not separate particles with absolute certainty, we expect some small amount of misidentification between pion and kaon that causes a reflection of $D^{\pm}$ under the $D_s^{\pm}$ peak (detailed work on the contamination has been reported in Ref. [9] measurement of D_s lifetime). Only resonant ($\phi\pi$, K^*K) channels were considered for this analysis to reduce the contribution of these reflections significantly. $D_s^{\pm}$ charm meson decays to $\phi\pi^{\pm}$ were selected by starting with candidate $\phi \to K^-K^+$ decays. The invariant mass for two well-reconstructed oppositely charged tracks, identified as kaons by RICH, was calculated. ϕ candidates were those pairs whose invariant mass was within ± 10 MeV/c^2 of the ϕ mass (1020 MeV/c^2). Similarly, those $KK\pi$ combinations that include a $K\pi$ pair with an invariant mass value within ± 35 MeV/c^2 of K^{0*} mass (892 MeV/c^2) were selected as $D_s^{\pm} \to K^{0*}(892)K^{\pm}$ decays. We have obtained 172 ± 14 D_s^- and 54 ± 8 D_s^+ in $\phi\pi$ channel and 174 ± 14 D_s^- and 71 ± 12 D_s^+ in K^*K channel for $x_F > 0.15$ with the Σ^- beam.

With the above cuts the $D_s^{\pm}$ peaks are clearly evident in the invariant mass spectra of $KK\pi^-$ and $KK\pi^+$ (Fig. 1). This figure also shows Cabibbo-suppressed $D^{\pm}$ peaks. There is a clear excess of D_s^- over D_s^+ as seen in the figure.

4. Production asymmetry and x_F analysis

Determining the yields through fitting the mass histograms for a specific x_F value by a Monte-Carlo generated shape is often inaccurate for small statistics and fluctuating backgrounds. In SELEX the yield at a specific x_F value was estimated using a sideband subtraction method assuming a linear background.
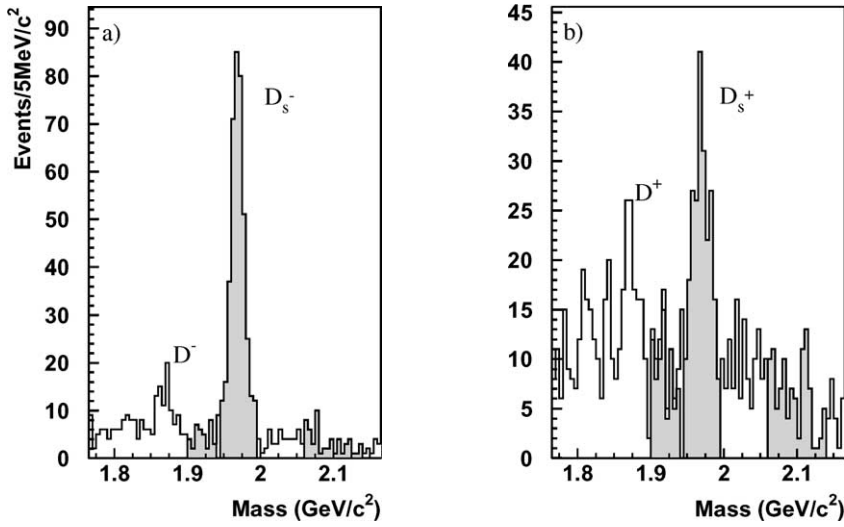
Fig. 1. Invariant mass distributions of (a) $KK\pi^-$ and (b) $KK\pi^+$ from the Σ^- beam. Mass interval and sidebands used in determining the yields for asymmetry calculations are shaded in both histograms. The data shown here include events having the decays $D_s^\pm \to \phi\pi^\pm$ or $K^*K^\pm$.

The mass ranges of the sideband background windows were [1.900 GeV/c^2, 1.940 GeV/c^2] and [2.060 GeV/c^2, 2.140 GeV/c^2]. We defined asymmetric sidebands to avoid the influence of $D^\pm \to K^+K^-\pi^\pm$ and to exclude the $D^*(2010)$ mass region.

The yields after sideband subtraction were corrected for the acceptance (reconstruction efficiency and geometrical acceptance) of the detector. To estimate the acceptance, D_s events were generated by a Monte Carlo program with a flat distribution in x_F and a Gaussian-distributed transverse momentum with mean $p_t = 0.8$ GeV/c. In a given simulation data set the D_s decays only into the K^*K or $\phi\pi$ mode. Decay tracks were digitized after smearing with detector resolution and multiple Coulomb scattering effects. The detector hits were OR'ed into the hit banks of interaction data. The new hit banks were passed through the SELEX off-line software. The acceptance was measured using the ratio of the reconstructed events to the embedded events. The set of cuts that was used to extract the signal was applied in this case as well. The most important issue for the asymmetry measurement was the relative efficiency of D_s^- and D_s^+.

As indicated in Fig. 2, the average difference in acceptance between D_s^- and D_s^+ is very small over all x_F range compared to the statistical uncertainty. This shows that the spectrometer is charge independent for D_s decay events. In the figure only the acceptance for
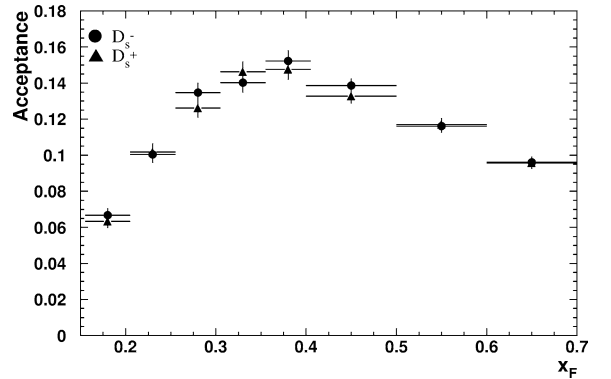

Fig. 2. Acceptances for D_s^- and D_s^+ obtained by embedding Monte Carlo events into data events. The acceptance here is the combination of geometrical acceptance and reconstruction efficiency of the $\phi\pi$ channel.

$\phi\pi$ channel is shown. The acceptance for K^*K channel is slightly lower. The acceptance in x_F is independent of p_t.

5. Results

After all the cuts and acceptance corrections, the resulting D_s yields as functions of x_F are shown in Fig. 3 and listed in Table 1. Resulting data points are

fit to a functional form $(1 - x_F)^n$. The values of n obtained from the fits are shown on the figure.

Since the beam flux was the same for $D_s^\pm$, the two distributions compare the relative production differential cross-sections for these states. Fig. 3 shows that, for the Σ^- beam used in this measurement, D_s^- production is favored over D_s^+ at all x_F, and the difference increases at large x_F.

We can discuss this difference in terms of an asymmetry parameter A, defined as

$$A \equiv \frac{N_{D_s^-} - N_{D_s^+}}{N_{D_s^-} + N_{D_s^+}}, \quad (1)$$

where $N_{D_s^-}$ and $N_{D_s^+}$ are the corrected yields for D_s^- and D_s^+, respectively. The asymmetry was calculated for five equally divided bins over an x_F range of 0.15 to 0.40 and for three equally divided bins over an x_F range of 0.40 to 0.70. Fig. 4 displays the acceptance-
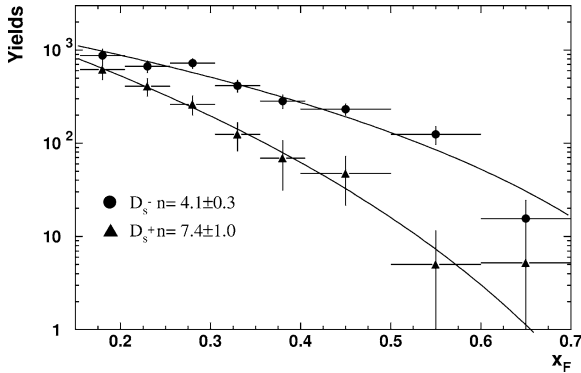
corrected asymmetry as a function of x_F for the Σ^- beam. It shows that there is a significant asymmetry in favor of D_s^- and that the asymmetry increases gradually as x_F increases. The asymmetry values are included in Table 1.

Fig. 5 displays the asymmetry as a function of p_t^2. These asymmetry values are also corrected for acceptance. One can see that the asymmetry is flat within the observed range up to $p_t^2 < 5 \ (\mathrm{GeV}/c)^2$.

In order to further explore the leading particle effect, the analysis was repeated with data from the π^- beam, obtained under the same conditions as with the Σ^- beam. Because pion beam statistics are much lower, we compare only integrated asymmetry results for all $KK\pi$ events with $x_F > 0.15$. For the
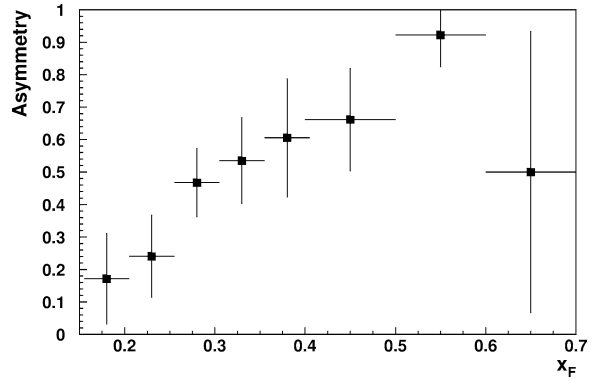

Fig. 3. Acceptance-corrected x_F distributions for D_s^- and D_s^+ from Σ^- beam. Fits of the yields to $(1 - x_F)^n$ for each charge state are plotted and the n-values listed.

Table 1
Summary of D_s^- and D_s^+ yields and asymmetries from Σ^- beam. The errors are statistical only. Yields are obtained from resonant state K*K and $\phi\pi$ events

x_F	$N_{D_s^-}$	$N_{D_s^+}$	Asymmetry
0.15–0.20	875 ± 156	619 ± 141	0.17 ± 0.14
0.20–0.25	669 ± 102	409 ± 91	0.24 ± 0.13
0.25–0.30	723 ± 92	262 ± 63	0.47 ± 0.11
0.30–0.35	413 ± 62	125 ± 43	0.54 ± 0.13
0.35–0.40	282 ± 49	69 ± 38	0.61 ± 0.18
0.40–0.50	232 ± 34	47 ± 26	0.66 ± 0.16
0.50–0.60	124 ± 28	5 ± 7	0.92 ± 0.10
0.60–0.70	15 ± 9	5 ± 5	0.50 ± 0.43

Fig. 4. Production asymmetry for Σ^- beam data as a function of x_F. Yields obtained from resonant (K*K and $\phi\pi$) events were used to calculate the asymmetry.
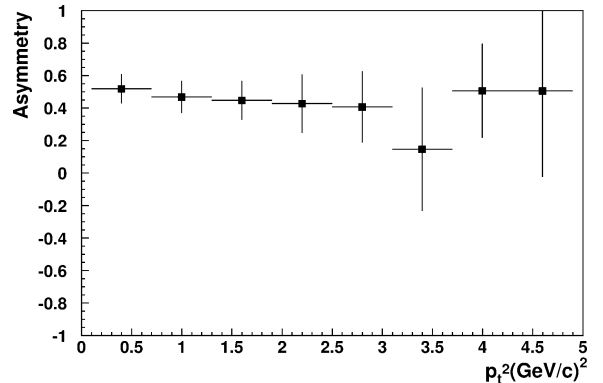

Fig. 5. Production asymmetry for Σ^- beam data as a function of p_t^2. Yields obtained from resonant (K*K and $\phi\pi$) events were used to calculate the asymmetry.

π^- beam, which has no leading particle, the integrated asymmetry is consistent with zero ($A = 0.06 \pm 0.11$). On the other hand, analysis of the Σ^- beam data in the same way results in a large asymmetry in favor of D_s^- ($A = 0.53 \pm 0.06$).

6. Systematic study

Studies of possible systematic errors due to the side-band subtraction method were done by varying the size and position of the side bands. Effects of changing x_F bin sizes on the results were also investigated. Systematics of the acceptance calculations have been checked with meson asymmetries and polarizations, all of which should be zero and are. The false asymmetry due to our hardware trigger was also studied. Even when combined together, these effects are all considerably smaller than the statistical uncertainty and are neglected. The contribution of the misidentification of π^- beam particles as Σ^- is estimated to be a few percent. The resulting dilution in the asymmetry is negligible.

As mentioned before, background including the $D^\pm$ contamination under the $D_s^\pm$ peak is highly reduced by limiting data to the resonant states. Effects of the remaining background were studied by comparing the integrated asymmetries obtained from the two resonant states. In the $\phi\pi$ case all backgrounds, including $D^\pm$ contamination, are negligible and cannot affect the asymmetry. The $\phi\pi$ integrated asymmetry is 0.52 ± 0.06. For the K*K channel it is 0.42 ± 0.08. The effect of the contamination reported in Ref. [9] would reduce a real K*K asymmetry of 0.52 to an observed value of 0.48, statistically compatible with observation. The overall dilution effect is much smaller than the statistical uncertainties in individual bins and is not included in the final results (Table 1 and Fig. 4).

7. Conclusion

To summarize: the $\Sigma^-(sdd)$ beam data show a strong production asymmetry favoring $D_s^-(\bar{c}s)$ production. This is consistent with leading particle effects. However, the integrated asymmetry from π^- beam at $x_F > 0.15$ for $D_s^\pm$ meson is 0.06 ± 0.11, which

is consistent with zero asymmetry as expected since neither D_s^+ nor D_s^- is a leading particle. Our Σ^- results are consistent with the previous measurement done by WA89 experiment at CERN with 340 GeV/c Σ^- beam.

The SELEX pion result of negligible integrated asymmetry agrees with the higher-statistics differential distribution for a 500 GeV π^- beam reported by E791 [4]. Their integrated asymmetry in the x_F range 0.1 to 0.5 is 0.032 ± 0.022. Our results also favor the color drag model over the intrinsic charm model, since the color drag model predicts a large asymmetry at large x_F independent of p_t [4,10,11].

References

[1] P. Nason, S. Dawson, K. Ellis, Nucl. Phys. B 327 (1989) 49.
[2] S. Frixione, M.L. Mangano, P. Nason, G. Ridolfi, Nucl. Phys. B 431 (1994) 453.
[3] WA89 Collaboration, M. Adamovich, et al., Eur. Phys. J. C 8 (1999) 593.

[4] E791 Collaboration, E.M. Aitala, et al., Phys. Lett. B 411 (1997) 230.

[5] F. Garcia, et al., Phys. Lett. B 528 (2002) 49.

[6] E. Norrbin, T. Sjostrand, Eur. Phys. J. C 17 (2000) 137.

[7] R. Vogt, S.J. Brodsky, Nucl. Phys. B 478 (1996) 311.

[8] J. Engelfried, et al., Nucl. Instrum. Methods A 431 (1999) 53.

[9] M. Iori, et al., Phys. Lett. B 523 (2001) 22.

[10] E769 Collaboration, G.A. Alves, et al., Phys. Rev. Lett. 72 (1994) 812;
E769 Collaboration, G.A. Alves, et al., Phys. Rev. Lett. 72 (1994) 1946, Erratum.

[11] E791 Collaboration, E.M. Aitala, et al., Phys. Lett. B 371 (1996) 157.